nature cell biology

Abi1 is essential for the formation and activation of a WAVE2 signalling complex

Metello Innocenti[1,3], Adriana Zucconi[1,3], Andrea Disanza[1,3], Emanuela Frittoli[1,3], Liliana B. Areces[1,3], Anika Steffen[5], Theresia E. B. Stradal[5], Pier Paolo Di Fiore[1,2,3], Marie-France Carlier[4] and Giorgio Scita[1,3]

WAVE2 belongs to a family of proteins that mediates actin reorganization by relaying signals from Rac to the Arp2/3 complex, resulting in lamellipodia protrusion. WAVE2 displays Arp2/3-dependent actin nucleation activity *in vitro*, and does not bind directly to Rac. Instead, it forms macromolecular complexes that have been reported to exert both positive and negative modes of regulation. How these complexes are assembled, localized and activated *in vivo* remains to be established. Here we use tandem mass spectrometry to identify an Abi1-based complex containing WAVE2, Nap1 (Nck-associated protein) and PIR121. Abi1 interacts directly with the WHD domain of WAVE2, increases WAVE2 actin polymerization activity and mediates the assembly of a WAVE2–Abi1–Nap1–PIR121 complex. The WAVE2–Abi1–Nap1–PIR121 complex is as active as the WAVE2–Abi1 sub-complex in stimulating Arp2/3, and after Rac activation it is re-localized to the leading edge of ruffles *in vivo*. Consistently, inhibition of Abi1 by RNA interference (RNAi) abrogates Rac-dependent lamellipodia protrusion. Thus, Abi1 orchestrates the proper assembly of the WAVE2 complex and mediates its activation at the leading edge *in vivo*.

Site-directed actin polymerization in response to signalling is at the origin of complex motile processes such as cell migration, neurite extension, and bud growth in yeast[1]. This is mediated by a family of proteins, including WASP, N-WASP and Scar/WAVE, that contain a VCA (verprolin-homology, cofilin-homology and acidic region) catalytic domain. This domain can bind to G-actin and the Arp2/3 complex, resulting in filament branching at the membrane[2]. Although the modes of WASP and N-WASP regulation have been elucidated[2], much less is known about WAVE proteins. For example, WAVE2 was found to bind activated Rac through IRSp53, which, in turn can stimulate WAVE2-nucleating activity, suggesting a positive mode of regulation[3]. Conversely, WAVE1 was reported to be maintained in an inactive state through its association with three other proteins: Nap1, PIR121 and HSPC300 (ref. 4). This complex is unable to stimulate actin polymerization *in vitro*. GTP-bound Rac relieves this inhibition by inducing the disassembly of the inhibitory Nap1–PIR121 sub-complex from the active WAVE1–HSPC300. Additional complexity to this mode of action is suggested by the observations that Abi1 and Abi2, two Abl-binding proteins[5,6] involved in Rac activation[7], were identified as interactors of WAVE1 (ref. 8). Moreover, removing the *Drosophila melanogaster* homologues of Abi1, WAVE, Nap1 and PIR121 by RNAi abolished formation of lamellipodia[9], providing genetic evidence for interactions among these proteins. In any case, it seems that WAVEs assemble into multi-molecular units to function *in vivo*.

How these complexes are assembled, localized and regulated *in vivo* is not known. Understanding how the activity of WAVE is regulated requires a detailed analysis of the topological/functional relationships of the various partners of WAVE within the complexes. Here we use a reductionist approach, involving the reconstitution and characterization of sub-complexes of WAVE, to provide insight into the essential protein–protein interactions that control WAVE activity. This approach emphasizes the role of Abi1 in the regulation of WAVE2.

To identify interactors of Abi1, proteins specifically bound to Abi1 immunoprecipitates were resolved by SDS–PAGE and then subjected to mass spectrometry (Fig. 1a). The proteins that were unambiguously identified were: nebulin; ninein; auto T antigen; PIR121 (ref. 10; also named KIAA1168 (ref. 11), CYFIP2 (ref. 12) and POP (ref. 13)); Sra-1 (ref. 14; also named KIAA0068 (ref. 11)); Nap1 (also named Nap125 (ref. 15), NCKAP1 (ref. 16) and KIAA0587); WAVE2; HSC70; and HSP70 (Fig. 1a; see Supplementary Information, Fig. S1a). Validation of PIR121, Nap1 and WAVE2 as interactors of Abi1 was obtained by co-immunoprecipitation experiments. Immunoprecipitation of endogenous Abi1 resulted in the co-precipitation of PIR121, Nap1 and WAVE2 (Fig. 1b). In addition, PIR121, Nap1 and Abi1 also associated with WAVE immunocomplexes in reciprocal co-immunoprecipitation experiments (Fig. 1b). Together with the finding that al0l four proteins co-fractionate in gel filtration experiments (see below), this indicates that they form a tight macromolecular complex *in vivo*. Notably, treatment of cells with epidermal growth factor (EGF) or platelet-derived growth factor (PDGF)/serum (data not shown), known to elicit actin

[1]IFOM Istituto FIRC di Oncologia Molecolare Via Adamello 16, 20134, Milan, Italy. [2]University of Milan, Medical School, 20122, Milan, Italy. [3]Department of Experimental Oncology, Istituto Europeo di Oncologia (IEO), Via Ripamonti 435, 20141, Milan, Italy. [4]Dynamique du Cytosquelette Laboratoire d'Enzymologie et Biochimie Structurales, C.N.R.S. 91198 Gif-sur -Yvette. France. [5]German Research Centre for Biotechnology (GBF), Department of Cell Biology, Mascheroder Weg 1, D-38124 Braunschweig, Germany.
Correspondence should be addressed to G.S. (e-mail: gscita@ifom-firc.it).

Published online: 28 March 2004; DOI:10.1038/ncb1105

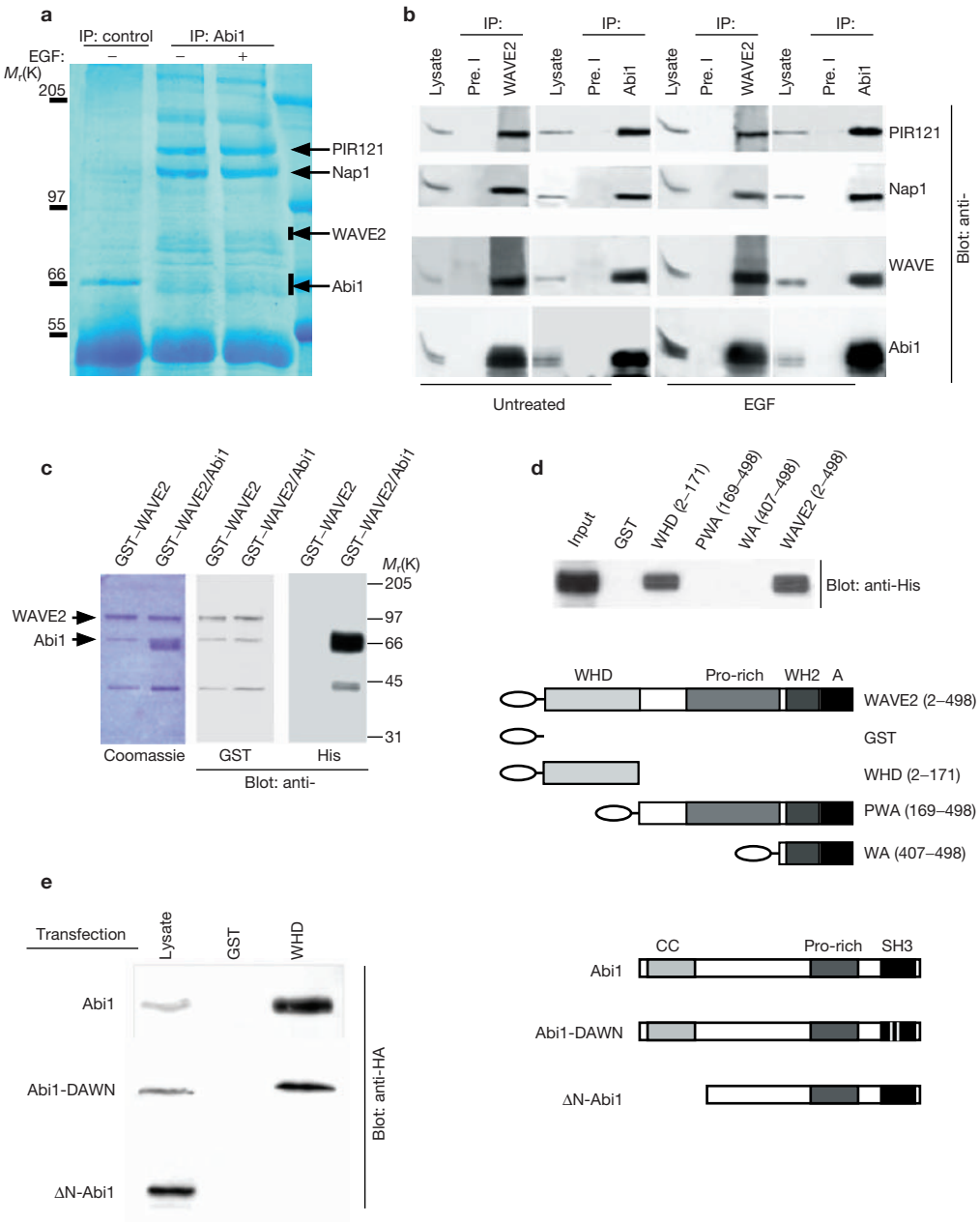

Figure 1 Abi1 binds to PIR121, Nap1 and WAVE2. (**a**) Pre-immune (IP: control) and Abi1 immunoprecipitates (IP: Abi), isolated from lysates of untreated (–) or EGF-treated (+) Cos-7 cells, were resolved by SDS–PAGE and stained with Brilliant Blue G Colloidal. The immunoaffinity purified bands were identified by MALDI spectrometry. PIR121, Nap1, WAVE2 and Abi1 are indicated. (**b**) Validation of PIR121, Nap1 and WAVE2 as Abi1 interactors. Lysates (1 mg) from HeLa cells, either untreated or treated with EGF, were immunoprecipitated with the indicated antibodies or the appropriate pre-immune sera. Lysates (20 μg) and immunoprecipitates were immunoblotted with the indicated antibodies. (**c**) Recombinant WAVE2 and Abi1 co-purify as a complex. Lysates of Sf9 cells, infected with GST–WAVE2 virus alone or together with His–Abi1 virus, were affinity purified using glutathione–agarose. The purified WAVE2 and WAVE2–Abi1 complex were visualized by Coomassie staining or immunoblotted with anti-GST or anti-His antibodies to detect GST–WAVE2 or His–Abi1, respectively. Molecular weight markers are shown on the right. (**d**) The WAVE2–Abi1 association is direct and mediated by the WHD domain of WAVE2. Binding of purified His–Abi1 to WAVE2 proteins (amino-acid boundaries are indicated) fused to GST or GST alone was detected by immunoblotting with an anti-His antibody. Shown are 30% of the input and 100% of the bound materials. A schematic representation of WAVE2 domain organization and of the WAVE2 fragments used is indicated. WHD, WAVE-homology domain; Pro-rich, proline-rich region; WH2, WASP-homologous domain 2; A, acidic region. (**e**) The N-terminal region of Abi1 is required for WAVE2 binding. Lysates from 293T cells transfected with the indicated HA–Abi1 proteins were incubated with GST alone or GST fused to the WAVE2 WHD domain. Lysates and bound proteins were immunoblotted with an anti-HA antibody. A schematic representation of Abi1 domain organization and of the Abi1 fragments used is indicated (CC, coiled-coil region; Pro-rich, proline-rich region; SH3, Src-homology 3 domain). Abi-DAWN, a version of Abi harbouring the mutations D453A and W455N.

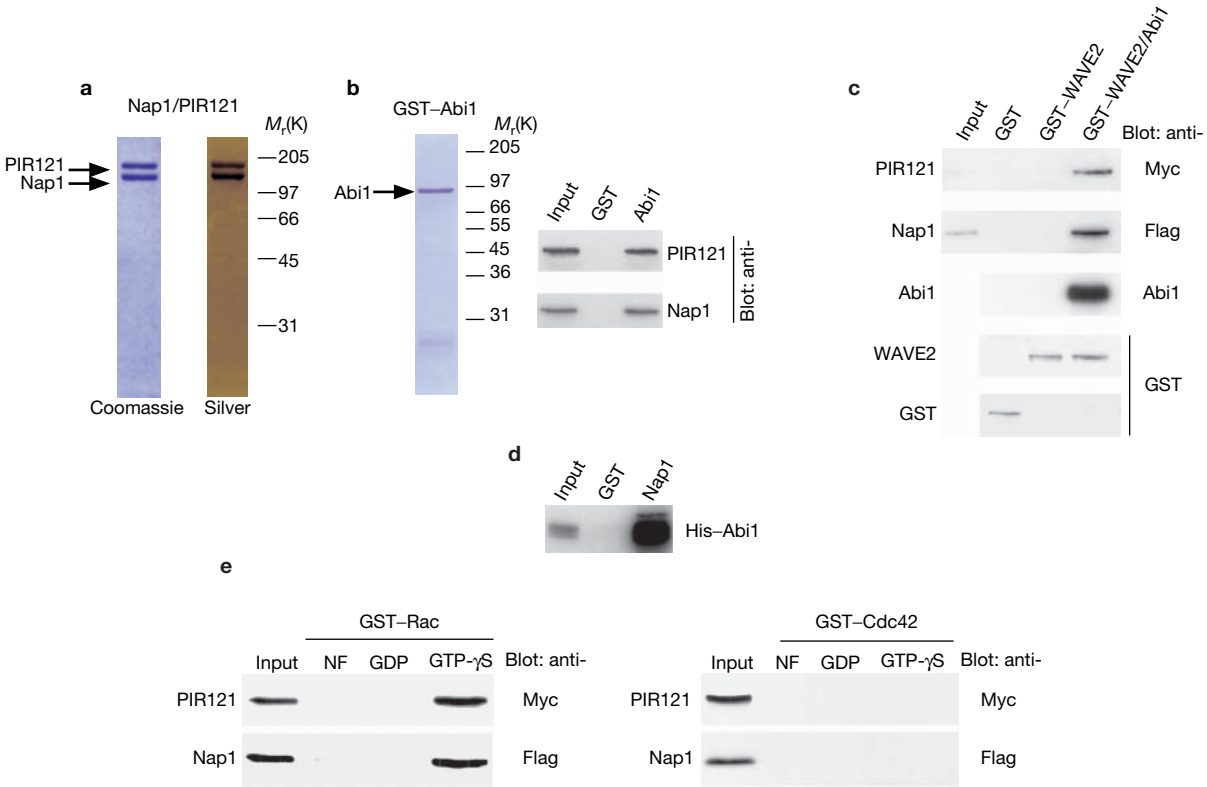

Figure 2 *In vitro* reconstitution of the WAVE2–Abi1–Nap1–PIR121 complex. (**a**) Coomassie and silver-stained gel of purified Nap1–PIR121 complex. Lysates from 293T cells co-transfected with Flag–Nap1 and Myc–PIR121 were subjected to immunopurification using agarose-conjugated anti-Flag IgG. Eluted proteins were stained with Coomassie Blue or silver staining. Flag–Nap1 and Myc–PIR121 migrated as 125K and 140K bands, respectively. (**b**) Recombinant and purified Abi1 associates with Nap1–PIR121. A Coomassie-stained gel of bacterially produced and purified GST–Abi1 is shown (left). Binding of the (Flag–Nap1)–(Myc–PIR121) complex to immobilized GST–Abi1 or GST alone was detected by immunoblot analysis with anti-Flag and anti-Myc antibodies, respectively (right). The input lane contains the (Flag–Nap1)–(Myc–PIR121) complex that was used for *in vitro* binding (20% of total). (**c**) Binding of the Nap1–PIR121 sub-complex to WAVE2 depends on Abi1. Immobilized GST–WAVE2, GST–WAVE2–Abi1 complex or GST alone were incubated with purified (Flag–Nap1)–(Myc–PIR121) complex. The input ((Flag–Nap1)–(Myc–PIR121) complex, 20% of total) and the affinity precipitated materials were immunoblotted with anti-Myc or anti-Flag antibodies to detect PIR121 and Nap1, respectively. An anti-GST antibody was used to detect GST and GST–WAVE2. Abi1 present in the WAVE2–Abi1 lane was detected with an anti-Abi1 antibody. (**d**) Recombinant and purified GST–Nap1 binds directly to Abi1. Binding of His–Abi1 to immobilized GST–Nap1 or GST was detected by immunoblot analysis with an anti-His antibody to detect Abi1. The input lane contains His–Abi1 used for the *in vitro* binding (5% of total). (**e**) GTP-loaded Rac, but not GTP-loaded Cdc42, binds to the Nap1–PIR121 complex. Binding of purified Nap1–PIR121 complex to immobilized, recombinant GST–Rac (left) or GST–Cdc42 (right). Rac and Cdc42 were depleted of nucleotide, loaded with GDP, or loaded with GTP-γS (see Methods). Bound proteins were detected by immunoblotting with anti-Flag and anti-Myc antibodies to detect Nap1 and PIR121, respectively. The input lane contained the (Flag–Nap1)–(Myc–PIR121) complex (20% of total).

polymerization[17], did not affect the association between PIR121, Nap1, WAVE and Abi1, indicating that the formation and stability of this complex are independent of stimuli resulting in actin remodelling (Fig. 1a, b).

To gain insight into the topological arrangement of the Abi1 complex, recombinant and purified proteins were used to reconstitute the complex *in vitro* and to map the interacting surfaces. Co-infection of insect cells with His–Abi1 and glutathione *S*-transferase (GST)–WAVE2 viruses followed by affinity precipitation using glutathione beads resulted in the co-purification of the two proteins (Fig. 1c). This interaction was mediated by the amino-terminal WAVE homology domain (WHD; Fig. 1d). Notably, the WHD domain of WAVE1 interacts equally well with purified His–Abi1 (see Supplementary Information, Fig. S1b, c), supporting the possibility that this region defines a new protein–protein interaction domain. Removal of 145 amino acids from the N terminus of Abi1 abrogated interaction with the WAVE2 WHD domain. The association of Abi1 with this WAVE2 domain was retained when the SH3-binding ability of Abi1 was impaired (Fig. 1e) or the entire proline-rich region and SH3 domain of Abi1 was removed (see Supplementary Information, Fig. S1d).

The direct association between WAVE2 and Abi1 suggests that these proteins may represent the backbone on which the other components then assemble. Nap1 and PIR121 are often found together in different multimolecular complexes[4,13,18,19]. In this study, these features were exploited to affinity purify these proteins as a sub-complex from 293T cells overexpressing Flag–Nap1 and Myc–PIR121, using immobilized anti-Flag antibodies. This resulted in the purification of a >95% pure Nap1–PIR121 complex (Fig. 2a). Recombinant and purified GST–Abi1 (Fig. 2b, left) associated directly with the Nap1–PIR121 sub-complex (Fig. 2b, right). Moreover, the preformed GST–WAVE2–Abi1 complex, but not GST–WAVE2 alone, bound

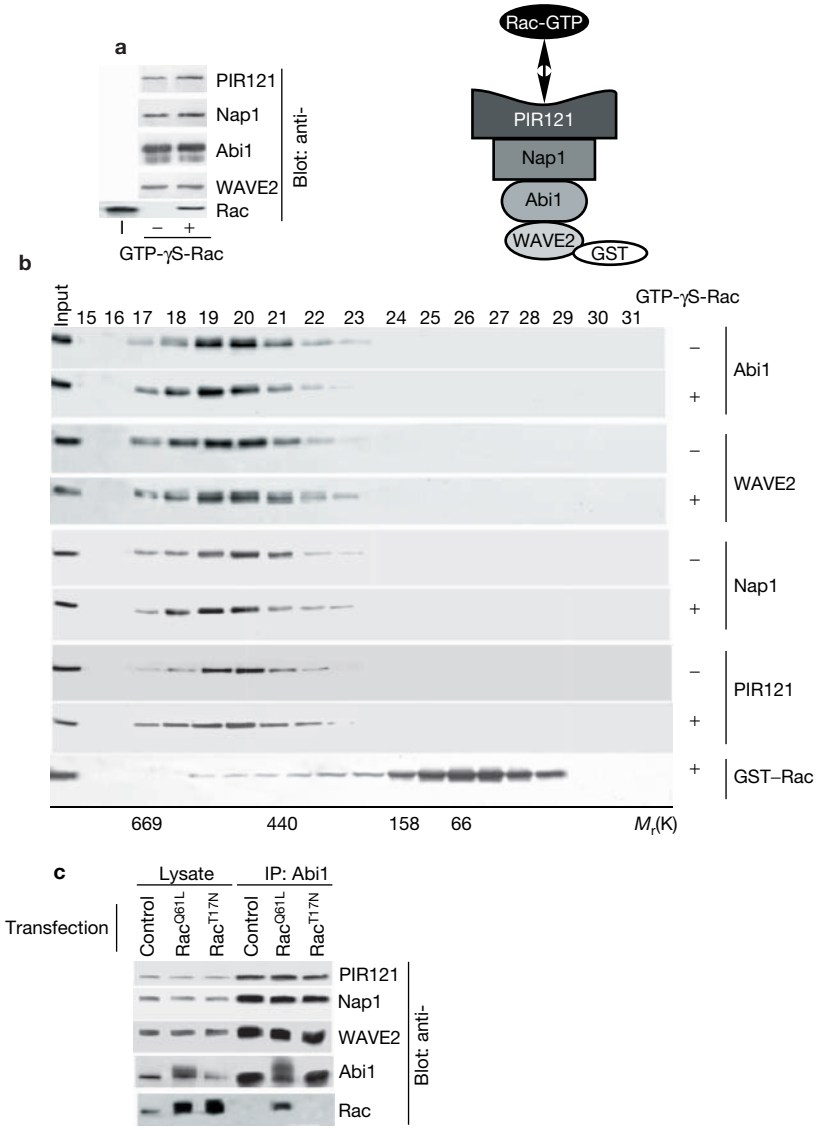

Figure 3 The WAVE–Abi1–Nap1–PIR121 complex is stable after GTP-γS-Rac binding. (**a**) GTP-loaded Rac binds to, but does not disrupt, the *in-vitro*-reconstituted WAVE2–Abi1–Nap1–PIR121 complex. Recombinant Rac loaded with GTP-γS (GTP-γS-Rac; 100 μM) was incubated with the pre-assembled GST–WAVE2–Abi1–Nap1–PIR121 complex (100 nM) immobilized on gluthatione beads. Bound proteins were immunoblotted with the indicated antibodies. Shown are 1% of the input and 100% of the bound material. (**b**) Gel-filtration chromatography of endogenous WAVE proteins, Abi1, Nap1 and PIR121 in the presence or absence of GTP-loaded Rac. Total cellular lysates of 293T cells (3.5 mg), incubated in the presence of GTP-γS-bound Rac^{Q61L} (+), or GST as a control (–), were applied onto a 200-ml prep grade Superose 6 column. An aliquot of each fraction (indicated at the top) was resolved by SDS–PAGE and immunoblotted with the indicated antibodies. The elution profile of proteins of known molecular weight is indicated at the bottom. The input lane contained 100 μg of total cellular lysates. (**c**) The association of endogenous WAVE proteins, Nap1 and PIR121 to Abi1 is not altered by the expression of activated or dominant-negative mutants of Rac. Total cellular lysates of 293T cells transfected with Rac^{T17N}, Rac^{Q61L} or empty vector as a control, were immunoprecipitated with anti-Abi1 antibody. Lysate and immunoprecipitates were immunoblotted with the indicated antibodies. More than 90% of cells expressed the transfected Rac constructs, as judged by immunofluorescence microscopy analysis (data not shown). Equal amounts of Abi1 were immunoprecipitated under the different experimental conditions. The electrophoretic mobility shift of Abi1 in the Rac^{Q61L} lane is caused by phosphorylation (data not shown).

directly to Nap1–PIR121 (Fig. 2c). Finally, purified His–Abi1 associated with GST–Nap1 (Fig. 2d), suggesting that Nap1 mediates the interaction of the Nap1–PIR121 complex to Abi1. Therefore, Abi1 is essential for the assembly of a WAVE2–Abi1–Nap1–PIR121 macromolecular complex.

In agreement with an earlier finding[18], the purified Nap1–PIR121 sub-complex associated specifically with recombinant GTP-γS-loaded Rac (Fig. 2e, left panels), but not with GTP-loaded Cdc42 (Fig. 2e, right panels). Moreover, no interaction was observed when Rac (or Cdc42) was in a nucleotide-free or a GDP-bound state (Fig. 2e). In addition, no binding between GTP-γS–Rac1 and Nap1 or the WAVE2–Abi1 complex could be detected (see Supplementary

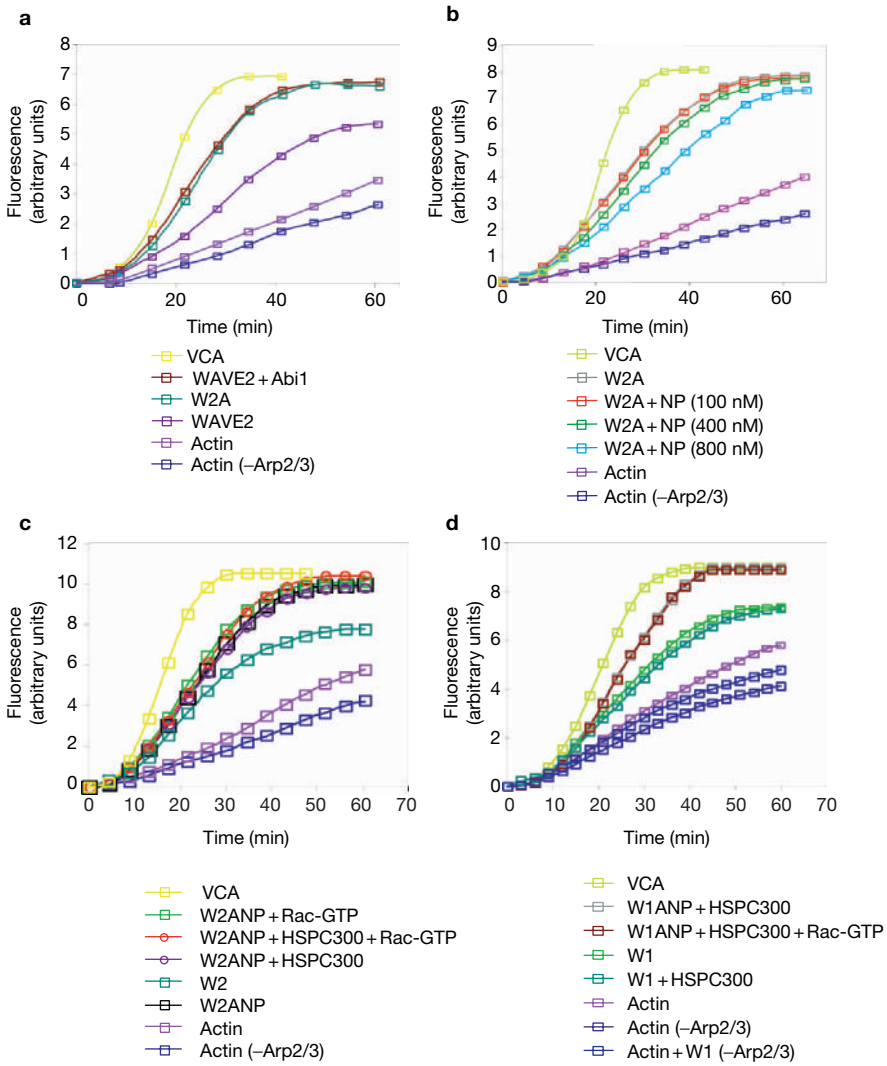

Figure 4 Stimulation of Arp2/3 by WAVE2 and WAVE1 is enhanced by Abi1. (**a**) Kinetics of Arp2/3-mediated polymerization in the presence of WAVE2, the VCA domain, WAVE2 and Abi1 added separately (WAVE2 + Abi1), and the WAVE2–Abi1 complex (W2A, 100 nM). (**b**) WAVE2–Abi1 complex (W2A, 100 nM) in the absence or presence of increasing concentration of the Nap1–PIR121 complex (NP; 100 nM, 400 nM and 800 nM). (**c**) WAVE2–Abi1–Nap1–PIR121 complex (W2ANP, 100 nM) in combination with GTP-γS-loaded GST–Rac1 (Rac-GTP, 2 μM), HSPC300 (100 nM), or Rac-GTP and HSPC300 together. (**d**) Kinetics of Arp2/3-mediated polymerization in the presence of WAVE1, WAVE1 + HSCP300, WAVE1–Abi1–Nap1–PIR121–HSPC300 complex (W1ANP + HSPC300), WAVE1–Abi1–Nap1–PIR121–HSPC300 complex + 2 μM of Rac-GTP (W1ANP + HSPC300 + RacGTP). Equimolar amounts (100 nM) of WAVE1, Abi1, Nap1, PIR121 and HSPC300 were used. The VCA domain of WAVE2 (100 nM), which displayed a reduced actin-polymerizing activity when compared with the VCA domain of N-WASP (see Supplementary Information, Fig. 4e), was used to activate Arp2/3, as a positive control. HSPC300, produced as a GST fusion protein, bound WAVE proteins directly (see Supplementary Information, Fig. 4f). The concentration of actin was 2.5 μM and that of the Arp2/3 complex was 10 nM.

Information, Fig. S1f). Therefore, the Nap1–PIR121 sub-complex links Rac to the WAVE2–Abi1 complex. Consistently, GTP-γS-loaded Rac could be recovered with the pre-assembled, immobilized GST–WAVE2–Abi1–Nap1–PIR121 complex (Fig. 3a, Methods). This indicates that unlike the WAVE1–Nap1–PIR121–HSPC300 heterotetramer (which dissociates after binding to GTP-loaded Rac[4]), the WAVE2–Abi1–Nap1–PIR121 complex is stable after addition of a 1,000-fold molar excess of activated Rac. To test whether the stability of the complex in the presence of GTP-loaded Rac is physiologically relevant, different experimental approaches were undertaken. First, analysis of the elution profile of total cellular lysates by size exclusion chromatography revealed that WAVEs, Abi1, Nap1 and PIR121 co-eluted at a relative molecular mass (M_r) of approximately 500,000 (500 K). The addition of GTP-loaded Rac to the lysates before gel filtration chromatography (Fig. 3b) or transfection with a constitutively active Rac (Rac^{Q61L}; see Supplementary Information, Fig. S2a) did not alter the elution profile of any of the components of the complex. Notably, the amount of activated Rac eluted with (Fig. 3b), or associated with (Fig. 3c), the endogenous WAVE–Abi1–Nap1–PIR121 complex was relatively small. However, this is expected when a protein is expressed to high levels through transient transfection or when an excess of recombinant protein is used. Similar findings were obtained when total cellular lysates from mouse brain (which express mainly the tissue specific WAVE1 and Abi2 proteins) were used[20,21]. This indicates that both WAVE1 and

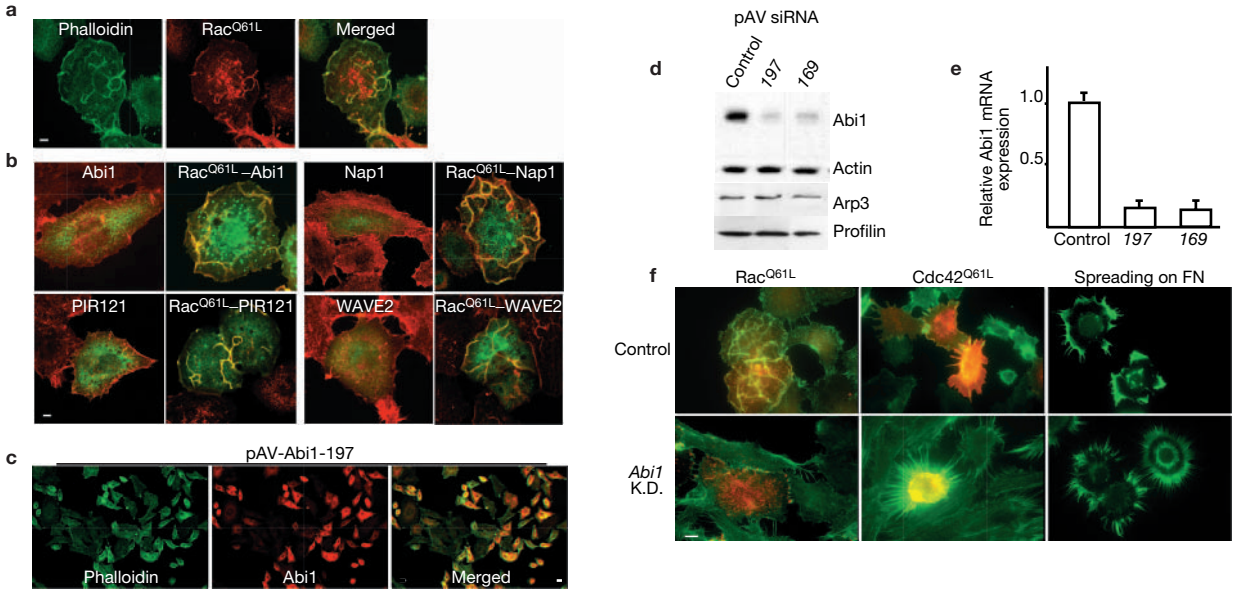

Figure 5 Abi1 is essential for Rac-dependent lamellipodia protrusions. (**a**) Rac-induced actin remodelling. HeLa cells transfected with HA–Rac^{Q61L} were serum starved, fixed and stained with an anti-HA antibody (Rac, red) and FITC–phalloidin to visualize F-actin (phalloidin, green). Colocalization of Rac and F-actin (yellow) is shown in the merged image. More than 90% of Rac^{Q61L}-expressing cells formed dorsal ruffles. (**b**) Re-localization of Abi1, WAVE2, Nap1 and PIR121 to Rac-induced ruffles. HeLa cells, transfected with GFP–Abi1, GFP–WAVE2, GFP–Nap1, or GFP–PIR121 alone or in combination with HA–Rac^{Q61L}, were fixed. GFP and F-actin were detected by epifluorescence (green), and by phalloidin staining (red), respectively. The expression of GFP fusion proteins and Rac^{Q61L} was assessed by staining with an anti-HA antibody (see Supplementary Information, Fig. 5). Endogenous Abi1 and WAVE2 accumulated into Rac^{Q61L}-induced lamellipodia (see Supplementary Information, Fig. 4g). Confocal apical sections are shown. (**c**–**e**) Silencing of *Abi1* by siRNA. (**c**) Stable suppression of *Abi1* gene expression in HeLa cells was obtained by co-transfecting pAV vectors (pAV-ctr or pAV-Abi1-197 or pAV-Abi1-169) with pBabe-puro plasmids. Cells were selected with 2.5 μg ml^{-1} puromycin, fixed and then stained to detect Abi1 antibody (red) and F-actin (green). A puromycin-selected mass population is shown. (**d**, **e**) Three representative stable clones (obtained by limiting dilution) for pAV-ctr (ctr) and pAV-Abi1-197 (*197*) and pAV-Abi1-169 (*169*) were analysed by immunoblotting with the indicated antibodies (**d**), or real-time, quantitative RT-PCR using specific Abi1 primers (**e**). Data, normalized to GAPDH or actin mRNA, are expressed relative to the levels of *Abi1* mRNA detected in control cells. (**f**) *Abi1* gene silencing abrogates Rac-mediated actin remodelling. Control and Abi1 knock-down (*Abi* K.D.) HeLa cells transfected with HA–Rac^{Q61L} (left) or HA–Cdc42^{Q61L} (centre) were fixed and stained with an anti-HA (red) antibody, and FITC-conjugated phalloidin. More than 90% of transfected cells displayed the actin cytoskeleton phenotypes shown. Control and Abi1 knock-down HeLa clones were plated on FN-coated coverslips (right). After various times, cells were fixed and stained for F-actin. Shown are cells fixed 180 min after plating. Scale bar represents 10 μm for all panels.

WAVE2 proteins associate stably in an Abi–Nap1–PIR121 complex (see Supplementary Information, Fig. S2b). Finally, ectopic expression of Rac^{Q61L} (Fig. 3c) or treatment with EGF (Fig. 1b; also see Supplementary Information, Fig. S3c–e) caused no reduction in the amount of WAVE, Nap1 or PIR121 co-immunoprecipitating with Abi1. Thus, WAVE, Abi1, Nap1 and PIR121 exist as a stable macromolecular complex both *in vitro* and *in vivo*.

Next, we tested the ability of recombinant WAVE2 and the reconstituted WAVE2 complex to activate Arp2/3, in a pyrene-labelled actin polymerization assay. Recombinant WAVE2 activated the Arp2/3 complex, and the addition of Abi1 significantly increased this activity (Fig. 4a). Conversely, addition of increasing amounts of the Nap1–PIR121 sub-complex had no effect on activation of the Arp2/3 complex induced by WAVE2 (data not shown) or WAVE2–Abi1 (Fig. 4b). Similarly, a reconstituted pre-assembled WAVE2–Abi1–Nap1–PIR121 complex attained the same activity as the WAVE2–Abi1 complex (data not shown). These results are in contrast to an earlier report, showing that WAVE1 is *trans*-inhibited when engaged in a complex containing Nap1, PIR121, HSPC300, and possibly Abi2 (ref. 4). To test whether the presence of HSPC300 and/or intrinsic differences between the two WAVE proteins (WAVE1 versus WAVE2) accounts for these discrepancies, we purified recombinant WAVE1 and HSPC300 and tested the actin polymerization activity of the reconstituted complexes containing either WAVE1–Abi1–Nap1–PIR121 or WAVE2–Abi1–Nap1–PIR121. Both WAVE2- and WAVE1-based complexes displayed Arp2/3-dependent actin-branching activity that was not significantly altered by the addition of HSPC300 (Fig. 4c, d). Thus, Abi1, but not HSPC300, Nap1 or PIR121, enhances the ability of WAVE proteins to stimulate Arp2/3 actin nucleation *in vitro*. However, the ability of PIR121 to mediate a direct interaction with Rac suggested that the activity of the WAVE2–Abi1–Nap1–PIR121 complex might be regulated after the binding of GTP-loaded Rac. At least two mechanisms can be envisioned: the complex might have a basal level of activity that is modulated after Rac binding to achieve physiological relevance; alternatively, Rac may regulate the complex *in vivo* by controlling its localization. For example, stimulation of Rac may recruit the complex to the leading edge of lamellipodia, where actin nucleation occurs. No modulation in the ability of WAVE proteins (data not shown) or the WAVEs–Abi1–Nap1–PIR121–HSPC300 complex to activate Arp2/3 could be observed after addition of a 20-fold molar excess of GTP-loaded Rac in polymerization assays *in vitro* (Fig. 4c, d). Conversely, transfection of HeLa cells with Rac^{Q61L}, or stimulation with EGF (see Supplementary Information, Fig. S3a), induced re-localization of WAVE2, Abi1, Nap1 and PIR121 to the leading edge of ruffles (Fig. 5a,

b), where they co-localize with Rac (see Supplementary Information, Fig. S3b). Thus, a scenario can be envisioned whereby a WAVE2–Abi1–Nap1–PIR121 complex exists *in vivo* and is recruited through a direct interaction with Rac to lamellipodia, where actin polymerization required for membrane protrusion is initiated and controlled.

By potentiating the activation of WAVE2 actin polymerization *in vitro*, and the assembly of WAVE-containing complexes *in vivo*, Abi1 is predicted to function in Rac-dependent actin remodelling. To test this, we employed a small-interfering RNA strategy to knock down Abi1 transcripts. Abi1 expression could be successfully ablated in HeLa cells transfected with siRNA-expressing vectors, as determined by immunofluorescence microscopy, immunoblotting and quantitative RT-PCR analysis (Fig. 5c, d). Analysis of the cyto-architecture of Abi1 knock-down cells indicated that they displayed an elongated morphology and an apparent reduction in the overall level of filamentous actin (see Supplementary Information, Fig. S3c). More importantly, they failed to undergo actin remodelling after expression of Rac^{Q61L}, supporting the notion that the Abi1-based complex is essential in this pathway (Fig. 5f). This was confirmed by the observations that actin remodelling in response to a variety of stimuli known to activate Rac was impaired in Abi1 knock-down cells. A constitutively active Cdc42 mutant ($Cdc42^{Q61L}$) regulates the formation of Rac-independent filopodia and Rac-dependent lamellipodia[22]. In Abi1 knock-down cells, no ruffles were induced by $Cdc42^{Q61L}$ expression, whereas the ability to form filopodia was retained (Fig. 5f). Similarly, Rac-dependent lamellipodia were completely absent in Abi1 knock-down cells after adhesion to extracellular matrix (ECM) proteins[23], such as fibronectin, and were able to spread on fibronectin by forming filopodia-like structures (Fig. 5f). Finally, no ruffling was observed in Abi1 knock-down cells in response to EGF treatment, which induced activation of Rac to levels similar to those observed in control cells (see Supplementary Information, Fig. S3d, e). A similar impairment in Rac-dependent membrane protrusion could also be observed after siRNA-mediated ablation of WAVE2 (see Supplementary Information, Fig. S3f–i), Nap1 or PIR121 (refs 9, 24). Interestingly, functional removal of either WAVE2 (Supplemental Information Fig. 4a) or Abi1 (see Supplementary Information, Fig. S4b) prevented the redistribution of other components of the complex to the leading edge of lamellipodia, indicating that the integrity of the complex is essential for its proper localization. Finally, in agreement with recent reports[9,24], blockade of Abi1 expression resulted in a substantial and specific down-regulation of WAVE2, Nap1 and PIR121 protein levels (see Supplementary Information, Fig. S4c), without affecting levels of their transcripts (data not shown). Therefore, Abi1 is also necessary for the stability of WAVE2, Nap1 and PIR121. In conclusion, the above data demonstrate that Abi1 is an essential component of WAVE2-containing signalling complexes and is required to mediate Rac-dependent actin remodelling.

Our results indicate that Abi1 is an essential component of WAVE-containing macromolecular assemblies. Abi1 positively regulates WAVE1 and WAVE2 activities *in vitro,* and connects WAVE2 to Rac through the assembly of a WAVE2–Abi1–Nap1–PIR121 complex. The WAVE2–Abi1–Nap1–PIR121 complex is recruited to lamellipodia after Rac activation, resulting in site-directed nucleation of actin filaments.

Binding of the WAVE(s)–Abi1–Nap1–PIR121 complex to Rac does not result in dissociation of the complex or affect its activity. These results are in contrast to recent findings, which reported that a WAVE1-containing complex purified from mouse brain is inactive and that binding of GTP-Rac causes disruption of the complex and activation of WAVE1 (ref. 4). Several possibilities may account for these differences. For example, the exact composition and structure of the complexes, either isolated from brain tissues or reconstituted from recombinant proteins, as well as their state of post-translational modification, might be different. In our hands, however, there was no evidence for GTP-Rac-induced dissociation of endogenous WAVE-based complexes isolated from a variety of cell lysates (Fig. 3; see Supplementary Information, Fig. S2a, b). We therefore favour the view that the WAVE complex is stable, active, and presumably able to bind Arp2/3 in the cytoplasm. However, the stimulation of actin assembly occurs only at the leading edge, raising the question of how WAVE-induced actin polymerization is controlled in a site-restricted fashion to elicit protrusion. In this respect, it should be noted that the actual branching process requires the association of a ternary, WAVE–G-actin–Arp2/3 complex to filaments to elicit branching, thus multiplying growing barbed ends. In quiescent cells, filaments exist but barbed ends are mostly capped[25], thereby preventing unwanted actin branching. Rac-dependent signalling results in the creation of new barbed ends by uncapping[25] and *de novo* nucleation, which is favoured by the increase in the steady-state concentration of G-actin that results from modulating the severing and depolymerizing activity of ADF–cofilin[26]. These Rac-dependent processes occur in a site-restricted fashion, and they must cooperate with Rac-induced localization of WAVE to the leading edge to elicit the generation and efficient growth of new filaments necessary to drive cell protrusion and motility. □

METHODS

Expression vectors, antibodies and cells. CMV (Cytomegalovirus)-promoter-based, EF (Elongation Factor-1α)-promoter-based eukaryotic expression vectors, and GST bacterial expression vectors were generated by recombinant PCR. HSPC300 was cloned by PCR from the UniGene Cluster Hs.421654. The pAV vector for suppression of gene expression was obtained by subcloning the H1-polymerase III-dependent promoter into a mammalian expression vector. Gene-specific targeting sequences were cloned 3′ of the H1 promoter. pFastBac-GST-WAVE2 (kindly provided by H. Miki; ref. 3) or pFastBac HT containing the Abi1 ORF (amino acid 2–480) were used as donors to generate recombinant bacmids according to Bac-to-Bac system (Invitrogen, Carlsbad, CA). All constructs were sequence verified. Flag–Nap1 was from A. Yamamoto[27]. Myc–PIR121 was a gift of A. Schenck and has been previously described[12]. pEGFP–Nap1 and pEGFP–PIR121 were from T. Stradal (GBF, Braunschweig, Germany). pGEX–WAVE1 was from L. Macheschy (Birmhingham, UK). The DAWN (D453A and W455N) mutant of Abi1, used in the experiments of Fig. 1e, is impaired in its ability to associate to its SH3-dependent ligands.

Antibodies were: rabbit polyclonal anti-Abi1[28], monoclonal anti-His (Santa Cruz Biotechnology, Santa Cruz, CA), anti-HA11 and anti-Myc 9E10 (Babco, Berkeley, CA), anti-Rac1 (Transduction Laboratories, Lexington, CA), rabbit polyclonal anti-Ds (RFP) (Clontech, Palo Alto, CA), monoclonal anti-Flag (Sigma, St Louis, MO), monoclonal anti-actin and profilin (Cytoskeleton, Denver, CO), rabbit polyclonal anti-Arp3 (Santa Cruz Biotechnology).

The monoclonal anti-Abi1 antibody was generated against the peptide PPVDYEDEEAAVVQYNDPYADGDPAWAPKNYI. Anti-Nap1 polyclonal serum recognizes a peptide spanning amino acids 1071–1085 (Eurogentec, Belgium). Polyclonal anti-PIR121/p140Sra, and anti-WAVE1 and anti-WAVE2 antibodies against specific peptides were from T. Stradal (GBF, Braunschweig). GST–WAVE2 (407–498) fusion protein of WAVE2 was used as an immunogen to obtain anti-PAN-WAVE polyclonal antibodies (also see supplementary information, Figs S1g and S3f). Where indicated, sera were affinity purified.

Abi1 knock-down HeLa cells were generated by transfecting pAV vectors coding for an Abi1-specific targeting sequence (pAV-Abi1-siRNA). Two distinct pAV-Abi1-siRNAs, spanning nucleotides 169–187 (pAV169) and 197–215 (pAV197) of human Abi1, respectively, were used. They were equally efficient in inhibiting Abi1 expression and resulted in similar phenotypic alteration. Control cells were obtained by transfecting a pAV vector coding a scrambled sequence. The generation of stable mass populations and single clones of Abi1 knock-down were obtained after puromycin-mediated selection of cells transfected

with pAV vectors together with plasmids carrying a puromycin resistance gene. At least six independently isolated Abi1 knockdown clones were analysed and showed similar results. Abi1 gene silencing could also be observed in transient experiments and caused a similar impairment in Rac-dependent actin remodelling (data not shown).

Mass spectrometry. Total cell lysates (40 mg) were immunoprecipitated with purified anti-Abi1 antibody, or control rabbit IgG coupled to Protein A–Sepharose. Proteins bound to the Abi1 immunocomplex were resolved by one-dimensional SDS–PAGE, visualized by Brilliant Blue G Colloidal (Sigma) staining, excised and then digested in the gel with trypsin, as described[29]. High-mass accuracy matrix-assisted laser-desorption ionization (MALDI) spectrometry was performed using a Voyager-DE BioSpectrometry workstation for MALDI time-of-flight mass spectrometer (PerSeptive Biosystems, Foster City, CA). Matrix-related ions and trypsin autolysis products were used for internal calibration. Delayed ion extration resulted in peptide masses with better than 35 ppm mass accuracy on average. Profound Peptide Mapping Software (Rockefeller University, version 4.10.5) was used to search a non-redundant protein sequence database (at the National Center for Biotechnology Information). The MALDI data were sufficient for the unambiguous identification of the proteins. In the case of WAVE2, nanoelectrospray peptide sequencing was also performed (see Supplementary Information, Fig. S1a).

Protein purification. His–Abi1, GST–WAVE2 and the GST–WAVE2–Abi1 complex were purified from Sf9 insect cells. Briefly, Sf9 cells infected with the appropriate viruses were lysed in 50 mM Tris-HCl at pH 8, 150 mM NaCl, 1 mM EDTA, 1 mM dithiothreitol, 5% glycerol, protease inhibitor cocktail (Roche, Basel, Switzerland), 1 mM NaF and 1 mM $NaVO_4$. GST–WAVE2 and GST–WAVE2–Abi1 complex were affinity purified using GS4B glutathione–Sepharose beads (Amersham Pharmacia Biotech, Piscataway, NJ). His–Abi1 was purified using Ni–NTA agarose (Qiagen) following standard procedures. Recombinant full-length Abi1, WAVE1, Nap1, Rac1, Cdc42 and WAVE2 fragments were all expressed as GST fusion proteins in BL21 *Escherichia coli* strain (Stratagene, Cedar Creek, TX). Abi1, produced either from insect cells (as a histidine-tagged protein) or from *E.coli* (as a GST fusion protein), displayed the same binding capability to its partners and similar activity for actin polymerization *in vitro*. Thrombin (Calbiochem-Novabiochem, San Diego, CA) was used to cleave GST from GST–Rac1, which was loaded with GDP or GTP-γS as described[7].

The PIR121–Nap1 sub-complex was affinity purified from 293T cells transfected with Flag–Nap1 together with Myc–PIR121 plasmids, using anti-Flag antibodies coupled to agarose beads (Sigma). Bound proteins were eluted with a Flag peptide (Sigma) according to the manufacturer's instructions. Eluted proteins were dialysed in 50 mM Tris-HCl, 150 mM NaCl, 1 mM dithiothreitol and 20% glycerol. PIR121–Nap1 and GST–WAVE2–Abi1 sub-complexes were quantified with respect to the molarities of Flag–Nap1 or GST–WAVE2, respectively.

In contrast to the Nap1–PIR121 complex, which was readily soluble and stable, purified Nap1 or PIR121 (derived from 293T cells overexpressing Flag–Nap1 or Myc–PIR121, respectively) was precipitated after the immunoaffinity purification. Nap1, but not PIR121, could be obtained from bacteria as a GST fusion protein (see Supplementary Information, Fig. S2).

Actin was isolated from rabbit muscles and purified in the Ca-ATP–G-actin form by Sephadex G-200 chromatography in G buffer (5 mM Tris-HCl at pH 7.8, 0.1 mM $CaCl_2$, 0.2 mM ATP, 1 mM dithiothreitol and 0.01% NaN_3). Actin was fluorescently labelled with pyrenil-iodoacetamide[30]. The C-terminal domain (VCA) of human N-WASP was expressed as a recombinant GST fusion protein and separated from GST by proteolytic cleavage[30]. The Arp2/3 complex was purified from bovine brain[30].

Biochemical assays. Standard procedures for protein analysis, *in vitro* binding, cell lysis and co-immunoprecipitation were as described[7].

Rac1 binding was measured by affinity precipitation as previously described[7], exploiting GST–CRIB (Cdc42- and Rac- interactive region) of PAK65 as a positive control.

Reconstitution of the PIR121–Nap1–Abi1–WAVE2 complex *in vitro* was obtained by incubating equimolar amounts of PIR121–Nap1 sub-complex and GST–WAVE2–Abi1 complex coupled to glutathione–agarose beads. Where indicated, equimolar amounts of HSPC300 were also added. The final concentration of each sub-complex in the mix was 100 nM. After a 1-h incubation and extensive washes, bound proteins were resolved by SDS–PAGE and visualized with appropriate antibodies. When Rac-GTP-γS was used, *in vitro* binding was performed in nucleotide-loading buffer[7] to preserve Rac loading.

For gel filtration analysis, 293T cells were lysed in 25 mM Tris-HCl at pH 7.6, 100 mM NaCl, 2 mM $MgCl_2$, 0.5 mM EGTA, 5% glycerol and 1% Triton X-100. Lysates were centrifuged at 15,000*g* for 20 min. Supernatants (3.5 mg total protein) were then applied on a 200-ml prep grade Superose 6 column equilibrated in 25 mM Tris-HCl at pH 7.6, 100 mM NaCl, 10 mM $MgCl_2$, 0.1 mM EGTA and 5% glycerol. The molecular weight of the eluted Abi1-based complex was judged by comparison with the elution profile of molecular weight standards. Aliquots of each fraction were resolved by SDS–PAGE and immunoblotted with the appropriate antibodies. When indicated, GTP-γS-loaded GST–Rac^{Q61L} or GST–Rac, or GST alone, were incubated at 4 °C with total cellular lysates in the presence of 10 mM $MgCl_2$ to preserve Rac loading before size exclusion chromatography. Notably, other known Abi1-binding partners, such as Eps8, Sos-1 and Abl, did not co-elute together with Abi1, indicating that they are not part of the WAVE2–Abi1–Nap1–PIR121 core complex.

Actin polymerization was monitored by the increase in fluorescence of 10% pyrenil-labelled actin. Polymerization was induced by addition of 0.1 M KCl, 1 mM $MgCl_2$ and 0.2 mM EGTA to a solution of Ca-ATP–G-actin containing Arp2/3 and the different proteins, as described in Fig. 4. Fluorescence measurements were performed at 20 °C in a Safax flx spectrofluorometer in which polymerization time courses of up to ten samples can be monitored simultaneously. Abi1, Nap1, PIR121 and HSPC300 had no effect on actin polymerization perfomed in presence of actin and Arp2/3 (see Supplementary Information, Fig. S4d).

Transfection and immunofluorescence microscopy. Cells seeded on gelatin were transfected with the indicated expression vectors using the LIPOfectamine reagent (Invitrogen), according to the manufacturer's instructions. After 48 h, cells were processed for epifluorescence or indirect immunofluorescence microscopy. Briefly, cells were fixed in 4% paraformaldehyde for 10 min, permeabilized in 0.1% Triton X-100 and 2% BSA for 10 min, and then incubated with the primary antibody for 45 min, followed by incubation with the secondary antibody for 30 min. F-actin was detected by staining with rhodamine-conjugated phalloidin (Sigma) at a concentration of 6.7 U ml^{-1}. Where indicated, cells were treated with EGF (100 ng ml^{-1}) for 10 min.
For spreading assays, Abi1 knock-down and the corresponding control cells were detached from the plate, incubated in medium containing 10% serum for 1 h before seeding on fibronectin-coated coverslips. Cells were fixed at different times and processed for indirect immunofluorescence microscopy to detect F-actin.

Note: Supplementary Information is available on the Nature Cell Biology website.

ACKNOWLEDGEMENTS
This work was supported by grants from AIRC (Associazione Italiana Ricerca sul Cancro) to G.S. and P.P.D.F.; Human Science Frontier Program to G.S. and M.F.C.; Telethon Foundation, the CNR (Target project Biotechnology) and the EC (V Framework) to P.P.D.F.; FIRC (Fondazione Italiana Ricerca sul Cancro) to M.I. from the Italian Ministry of Health to G.S. We would like to thank L. Cairns and S. Bossi for technical help, S. Polo for reading the manuscript, B. Baum for sharing unpublished materials, and G. Cesareni for helping with the generation of WAVE2 reagents.

COMPETING FINANCIAL INTERESTS
The authors declare that they have no competing financial interests.

Received 12 December 2003; accepted 5 February 2004

1. Pollard, T. D. The cytoskeleton, cellular motility and the reductionist agenda. *Nature* **422,** 741–745 (2003).
2. Takenawa, T. & Miki, H. WASP and WAVE family proteins: key molecules for rapid rearrangement of cortical actin filaments and cell movement. *J. Cell Sci.* **114,** 1801–1809 (2001).
3. Miki, H., Yamaguchi, H., Suetsugu, S. & Takenawa, T. IRSp53 is an essential intermediate between Rac and WAVE in the regulation of membrane ruffling. *Nature* **408,** 732–735 (2000).
4. Eden, S., Rohatgi, R., Podtelejnikov, A. V., Mann, M. & Kirschner, M. W. Mechanism of regulation of WAVE1-induced actin nucleation by Rac1 and Nck. *Nature* **418,** 790–793 (2002).
5. Shi, Y., Alin, K. & Goff, S. P. Abl-interactor-1, a novel SH3 protein binding to the

carboxy-terminal portion of the Abl protein, suppresses v-abl transforming activity. *Genes Dev.* **9,** 2583–2597 (1995).
6. Dai, Z. & Pendergast, A. M. Abi-2, a novel SH3-containing protein interacts with the c-Abl tyrosine kinase and modulates c-Abl transforming activity. *Genes Dev.* **9,** 2569–2582 (1995).
7. Scita, G. *et al.* EPS8 and E3B1 transduce signals from Ras to Rac. *Nature* **401,** 290–293 (1999).
8. Soderling, S. H. *et al.* The WRP component of the WAVE-1 complex attenuates Rac-mediated signalling. *Nature Cell Biol.* **4,** 970–975 (2002).
9. Rogers, S. L., Wiedemann, U., Stuurman, N. & Vale, R. D. Molecular requirements for actin-based lamella formation in Drosophila S2 cells. *J. Cell Biol.* **162,** 1079–1088 (2003).
10. Saller, E. *et al.* Increased apoptosis induction by 121F mutant p53. *EMBO J.* **18,** 4424–4437 (1999).
11. Nagase, T. *et al.* Prediction of the coding sequences of unidentified human genes. XII. The complete sequences of 100 new cDNA clones from brain which code for large proteins *in vitro*. *DNA Res.* **5,** 355–364 (1998).
12. Schenck, A., Bardoni, B., Moro, A., Bagni, C. & Mandel, J. L. A highly conserved protein family interacting with the fragile X mental retardation protein (FMRP) and displaying selective interactions with FMRP-related proteins FXR1P and FXR2P. *Proc. Natl Acad. Sci. USA* **98,** 8844–8849 (2001).
13. Witke, W. *et al.* In mouse brain profilin I and profilin II associate with regulators of the endocytic pathway and actin assembly. *EMBO J.* **17,** 967–976 (1998).
14. Kobayashi, K. *et al.* p140Sra-1 (specifically Rac1-associated protein) is a novel specific target for Rac1 small GTPase. *J. Biol. Chem.* **273,** 291–295 (1998).
15. Kitamura, T. *et al.* Molecular cloning of p125Nap1, a protein that associates with an SH3 domain of Nck. *Biochem. Biophys. Res. Commun.* **219,** 509–514 (1996).
16. Suzuki, T. *et al.* Molecular cloning of a novel apoptosis-related gene, human Nap1 (NCKAP1), and its possible relation to Alzheimer disease. *Genomics* **63,** 246–254 (2000).
17. Ridley, A. J., Paterson, H. F., Johnston, C. L., Diekmann, D. & Hall, A. The small GTP-binding protein rac regulates growth factor-induced membrane ruffling. *Cell* **70,** 401–410 (1992).
18. Kitamura, Y. *et al.* Interaction of Nck-associated protein 1 with activated GTP-binding protein Rac. *Biochem. J.* **322,** 873–878 (1997).
19. Soto, M. C. *et al.* The GEX-2 and GEX-3 proteins are required for tissue morphogenesis and cell migrations in *C. elegans*. *Genes Dev.* **16,** 620–632 (2002).
20. Soderling, S. H. *et al.* Loss of WAVE-1 causes sensorimotor retardation and reduced learning and memory in mice. *Proc. Natl Acad. Sci. USA* **100,** 1723–1728 (2003).
21. Benachenhou, N., Massy, I. & Vacher, J. Characterization and expression analyses of the mouse Wiskott-Aldrich syndrome protein (WASP) family member Wave1/Scar. *Gene* **290,** 131–140 (2002).
22. Hall, A. Rho GTPases and the actin cytoskeleton. *Science* **279,** 509–514 (1998).
23. Adams, J. C. Regulation of protrusive and contractile cell-matrix contacts. *J. Cell Sci.* **115,** 257–265 (2002).
24. Steffen, A. K. R., Ehinger, J., Innocenti, M., Scita, G., Wehland, J. & Stradal, T. E. B. Sra-1 and Nap1 link Rac to actin assembly driving lamellipodia formation. *EMBO J.* **23,** 749–759 (2004).
25. Allen, P. G. Actin filament uncapping localizes to ruffling lamellae and rocketing vesicles. *Nature Cell Biol.* **5,** 972–979 (2003).
26. Ichetovkin, I., Grant, W. & Condeelis, J. Cofilin produces newly polymerized actin filaments that are preferred for dendritic nucleation by the Arp2/3 complex. *Curr. Biol.* **12,** 79–84 (2002).
27. Yamamoto, A., Suzuki, T. & Sakaki, Y. Isolation of hNap1BP which interacts with human Nap1 (NCKAP1) whose expression is down-regulated in Alzheimer's disease. *Gene* **271,** 159–169 (2001).
28. Biesova, Z., Piccoli, C. & Wong, W. T. Isolation and characterization of e3B1, an eps8 binding protein that regulates cell growth. *Oncogene* **14,** 233–241 (1997).
29. Shevchenko, A., Wilm, M., Vorm, O. & Mann, M. Mass spectrometric sequencing of proteins silver-stained polyacrylamide gels. *Anal. Chem.* **68,** 850–858 (1996).
30. Pantaloni, D., Boujemaa, R., Didry, D., Gounon, P. & Carlier, M. F. The Arp2/3 complex branches filament barbed ends: functional antagonism with capping proteins. *Nature Cell Biol.* **2,** 385–391 (2000).